

# Positioning an electric wheelchair in 2D grid map based on natural landmarks for navigation using Q-learning

**Ba-Viet Ngo, Thanh-Hai Nguyen**

Department of Electronics-Biomedical Engineering, Faculty of Electrical and Electronics Engineering,  
Ho Chi Minh City University of Technology and Education, Ho Chi Minh City, Vietnam

---

## Article Info

### Article history:

Received Jan 19, 2023

Revised Feb 18, 2023

Accepted Mar 13, 2023

---

### Keywords:

2D grid map

Natural landmark

Positioning wheelchair

Q-learning

Wheelchair navigation

---

## ABSTRACT

Self-mobility electric wheelchairs are very useful for people with disabilities, so they can move without help in indoor environments. To create one self-mobility electric wheelchair, modern methods for control such as computer vision and machine learning can be applied. In particular, this electric wheelchair can move from any position in the indoor environment to the desired destination. For accuracy, natural landmarks are used and the navigation of the wheelchair is determined using a Q-learning reinforcement learning algorithm. In particular, this algorithm is applied to find the best path for the wheelchair to reach the destination. The article proposes a method to build one 2D grid map for wheelchair movement based on natural landmarks in the indoor environment. The new point of this method is that the position of the wheelchair can be accurately determined from a certain landmark instead of many landmarks applied in traditional methods. Some practical experiments were performed to illustrate the effectiveness of the proposed method in the indoor environment. This proposed method can be developed in more complex environments with natural landmarks.

*This is an open access article under the [CC BY-SA](https://creativecommons.org/licenses/by-sa/4.0/) license.*



---

## Corresponding Author:

Thanh-Hai Nguyen

Department of Electronics-Biomedical Engineering, Faculty of Electrical and Electronics Engineering

Ho Chi Minh City University of Technology and Education

01 Vo Van Ngan Street, Linh Chieu Ward, Thu Duc City, Ho Chi Minh City, Vietnam

Email: nthai@hcmute.edu.vn

---

## 1. INTRODUCTION

In recent years, smart wheelchair systems have been developed to assist people with disabilities [1]-[3]. Researches often focuses on three main areas: i) improvement of assistive technology; ii) improving physical user interface; and iii) improving control sharing between user and machine. A smart wheelchair can assist the elderly or severely disabled people during movement without help. This assistance significantly improves their life quality. Moreover, wheelchairs are designed to be able to make navigational decisions during movement of disabled people. Another research is that wheelchairs can help users move from one position to another one based on a map. In particular, the first stage of the mobility planning process is positioning to determine the coordinates of the wheelchair in 2D or 3D space. The second stage is to define and represent the movement trajectories for each different space suitable to each application. The final stage is navigation, in which the wheelchair can be manipulated to move based on current position. These three basic stages are the necessary steps in the self-propelled wheelchair to make independent movement without any assistance [4].

One of the most important problems of self-propelled wheelchairs is the positioning process. This problem is to determine the current position of the wheelchair in space. Positioning methods for wheelchairs or robots include: i) relative positioning (local positioning) of the wheelchair's position relative to the initial position. The advantage of this method is the fast computation speed without other information about the description of the

moving space; ii) absolute positioning (global positioning) of the wheelchair's position based on the global coordinate system through descriptions of the moving space; and iii) probabilistic positioning by combining both relative and absolute positioning methods to increase accuracy. Each method has its own advantages and disadvantages and is applied in different applications [5]. In the positioning algorithm, information about the surrounding environment needs to be collected accurately dependent on the sensor type.

Ultrasonic sensors were used first and most commonly in positioning for robots or electric wheelchairs [6]. With this type of sensor, the distances from the wheelchair or robot to the surrounding objects are continuously collected during movement. Therefore, these distances are calculated to find out which points lie on a straight line and compared with the available map for calculating the current position of the wheelchair or robot. However, this method is only used to identify large objects in the same plane with the sensor beam. Furthermore, the errors of methods using ultrasonic sensors are large and highly dependent on the number of sensors placed around the wheelchair or robot. Laser sensors have been used to replace ultrasonic sensors in a number of distance measurement applications [7]. Moreover, the laser sensors have a larger measuring range than that of the ultrasonic sensors and a higher resolution. However, ultrasonic or laser sensors cannot recognize landmarks and this is one of the major challenges in the positioning process. Therefore, it is necessary to use another type of sensor capable of collecting more different types of information such as a camera system [8].

Image sensors and image processing methods are being widely used for the localization of mobile platforms in natural environments with different landmarks. In practice, it is possible to create artificial landmarks in the dynamic environment for the robot to reach the desired destination [9], [10]. In the studies for mobile robots based on landmarks [11], [12], the robots can be designed to move in the natural environments with landmarks such as lights on the ceiling. With environments without dynamic structures such as industrial areas, offices, universities, where there are many natural landmarks, mobile robots can position themselves to move based on 3D data [13]. Chai *et al.* [14] introduced a method to localize mobile robots by identifying straight lines and uniform colors in a natural environment. In this environment, with characteristic regions, the method was applied to identify objects with natural landmarks for their orbits.

To detect objects in the image, the sub regional method was used for the recognition using the Sliding Window method [15], [16]. In addition, region proposal (RP) method has been applied to detect objects in images in recent years [17], [18]. This method can process an image to create bounding boxes corresponding to all patches as objects. Furthermore, RP can allow processing objects in an image with noise or overlap to produce proposed objects which are very close to the actual objects in that image. Therefore, the proposed object regions are classified based on the large density of features at the positions of the objects in the image, where the adjacent regions are grouped based on several characteristics such as color or texture. It is obvious that, thousands of proposed regions are rearranged to reduce the number of objects in the image [19]-[21].

Currently, the strong development of image processing algorithms possibly allows to determine distances from the camera systems installed with robots to objects through geometric projections from 3D space to 2D space and inversely [22]-[26]. The application of identifying natural landmarks to the positioning process has become increasingly popular in recent years. This paper proposes a positioning system based on natural landmarks and a camera system for an electric wheelchair navigation in the indoor environments to determine the wheelchair's position on a 2D grid map. In particular, landmarks are detected during navigation and then calculated to show the wheelchair's position and orientation on the map. The Q-learning algorithm is applied to provide a route so that the wheelchair can safely reach the desired destination. The structure of the article is as follows: section 2 represents the proposed method for positioning the wheelchair on one 2D grid map based on natural landmarks; in section 3, the experiments were performed and discussed about the obtained results; and section 4 provides conclusions about the proposed and the experimental results.

## 2. METHOD

In this study, a landmark system is built for positioning the electric wheelchair in a 2D grid map for navigation. In particular, the positions of natural landmarks are determined and stored in a database for positioning the wheelchair based on the cells in the 2D grid map and its coordinates. It means that directions will be determined for wheelchair mobility.

### 2.1. The system of natural landmarks

Images with natural landmarks often contain many features. Therefore, when a wheelchair installed with a stereo camera system for detecting similar landmarks in the real environment during movement is necessary. In particular, only the selected natural landmarks have the best outstanding features similar to those of the landmarks in the databased [19]. With the selected landmarks as shown in Figure 1, their location information will also be stored in the database to serve for the process of positioning the moving electric wheelchair. During the wheelchair's movement in the real environment with previously selected landmarks, if

the camera detects these landmarks, it will provide information about the location of the landmark relative to the camera position as shown in Figure 2. Furthermore, the distance from the camera to the detected landmark will be calculated under suitable lighting conditions. From Figure 2, the distance  $d$  from the camera center to the center of the landmark is calculated as:

$$d = \sqrt{x_a^2 + z_a^2} \tag{1}$$

in which  $z_a$  is the distance from the camera to the plane containing the landmark, with the spatial coordinate (OXYZ),  $x_a$  is the deviation of the landmark center to from the camera center, where the far value  $x_a > 0$ , if the landmark is the right side of the camera and  $x_a < 0$  if the landmark is the left of the camera.



Figure 1. Samples of landmarks in the indoor environment

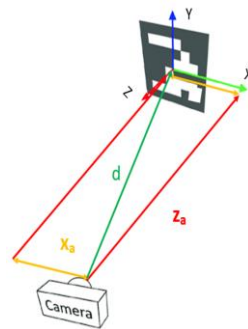


Figure 2. Coordinate system of the RGB-D camera

**2.2. Positioning the electric wheelchair in one 2D grid map**

Figure 3 shows the OXY coordinate system in the 2D plan and the camera coordinate system O'X'Y'. To know the position of the wheelchair in the 2D plane, the information from the camera's O'X'Y' coordinate system needs to be converted to the OXY coordinate system. Furthermore,  $(X_M, Y_M)$  is the coordinate of the landmark in the 2D plane and is usually determined based on landmarks.

In this article, the position of the wheelchair in the 2D plane according to the OXY coordinate system is calculated in 4 cases as described in Figures 3(a)-3(d) as follows:

- The direction of the landmark is Up in the 2D grid map shown in (2):

$$\begin{aligned} X_W &= X_M - x_a \\ Y_W &= Y_M - z_a \end{aligned} \tag{2}$$

- The direction of the landmark is Down in the 2D grid map shown in (3):

$$\begin{aligned} X_W &= X_M + x_a \\ Y_W &= Y_M + z_a \end{aligned} \tag{3}$$

- The direction of the landmark is Right in the 2D grid map shown in (4):

$$\begin{aligned} X_W &= X_M - z_a \\ Y_W &= Y_M + x_a \end{aligned} \tag{4}$$

– The direction of the landmark is Left in the 2D grid map shown in (5):

$$\begin{aligned} X_W &= X_M + z_a \\ Y_W &= Y_M - x_a \end{aligned} \tag{5}$$

in which  $(X_W, Y_W)$  is the coordinate of the wheelchair in the OXY plane;  $(X_M, Y_M)$  is the coordinate of the landmark in the OXY plane;  $x_a$  is the deviation from the center of the camera to that of the landmark;  $z_a$  is the distance from the center of the camera to the plane containing the landmark.

After obtaining the position of the wheelchair in the OXY plane, the wheelchair position in the 2D grid map will be determined. Assuming that a 2D grid map as shown in Figure 3(e) has the size of each cell  $(a \times a)$  and its origin  $(0,0)$  is at the top left corner, the position of the wheelchair  $(X_G, Y_G)$  in the 2D Grid map is calculated using the following (6):

$$\begin{aligned} X_G &= n - \text{round}\left(\frac{Y_W}{a}\right) \\ Y_G &= \text{round}\left(\frac{X_W}{a}\right) - 1 \end{aligned} \tag{6}$$

in which  $n$  is the total number of cells along the vertical axis of the 2D Grid map.

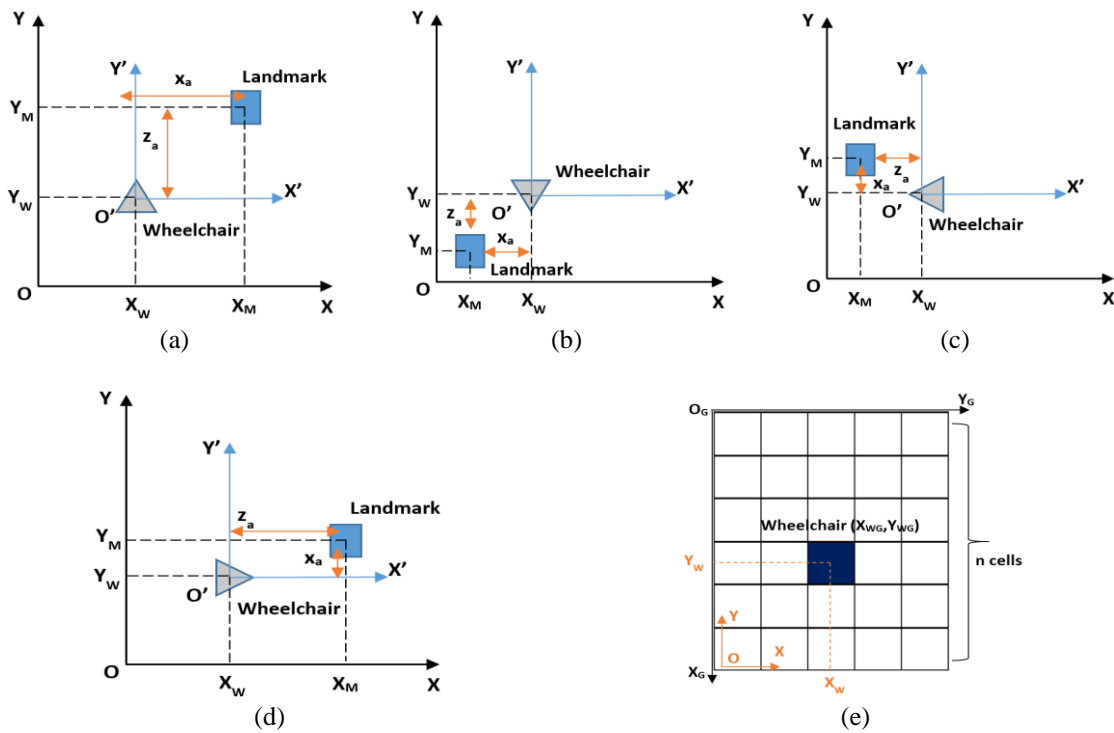


Figure 3. Positions of the wheelchair with four directions: (a) up direction of landmark, (b) down direction of landmark, (c) left direction of landmark, (d) right direction of landmark, and (e) the 2D grid map and in the OXY plane

### 2.3. Navigation of the electric wheelchair based on natural landmarks and Q-learning

Figure 4 depicts a real wheelchair control model based on the Q-learning method and landmarks. In this model, the wheelchair will be positioned on the 2D grid map through the landmarks, including the position and orientation of the wheelchair. Only the wheelchair position is calculated in Q-learning for determining the movement route and producing specific actions for the wheelchair's state. The wheelchair's direction  $d$  relative to the 2D grid map origin will feed into a block for converting the predicted activities from the Q-learning  $a$  (Up, Down, Left, Right) into actual actions for the wheelchair's movement  $a_w$  (forward, backward, left-forward, right-forward) because the electric wheelchair is not an omnidirectional control model [27]. Specifically, for a starting point and a destination point on a 2D grid map, the Q-learning method will produce a series of actions. These actions will be converted into actual actions and sent to the controller. Thus, the wheelchair can move along an optimal route from the starting position to the destination position.

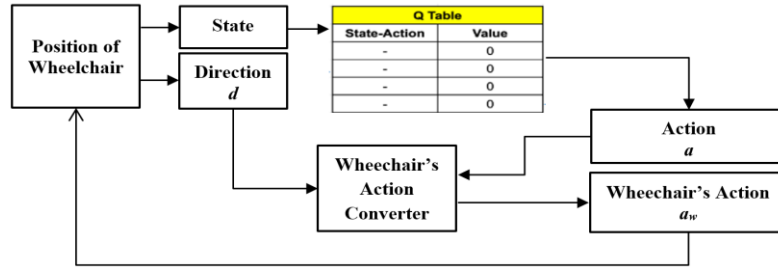


Figure 4. A real wheelchair control model based on Q-learning

Q-learning is the reinforcement learning policy that will find the next best action based on the current state [28]. In particular, it randomly chooses an action to maximize rewards. Furthermore, Q-learning is the reinforcement learning method without a model and off-policy, but it can find the best action direction based on the agent’s current state. This means that it depends on the agent’s position in the environment and the algorithm will decide the next action to work out. In addition, Q-learning is the learning algorithm based on the updated value function of the Bellman equation, in which the value, called Q, is calculated using the as shown in (7):

$$Q(s, a) = r(s, a) + \gamma \max_a Q(s', a) \tag{7}$$

in which  $Q(s,a)$  is the  $Q$  value when performing action  $a$  at the state  $s$ ;  $r(s,a)$  is the received reward;  $s'$  is the next state,  $\gamma$  is the discount factor, ensuring that the far away from the destination, the smaller the  $Q$  value.

From (7), a state-action matrix  $Q$  can be created as a lookup table. Therefore, each agent state only needs to find the action with the largest  $Q$  value. However, the  $Q$  value before and after the action will be different, and this difference is called the temporal difference (TD) [29] and is described as (8):

$$TD(s, a) = r(s, a) + \gamma \max_{a'} Q(s', a') - Q_{t-1}(s, a) \tag{8}$$

Thus, with the times the agent performs actions,  $Q(s, a)$  will gradually converge and this process is Q-learning. Therefore, the matrix  $Q$  needs to update the weights based on TD using the shown in (9):

$$Q_t(s, a) = Q_{t-1}(s, a) + \alpha TD_t(s, a) \tag{9}$$

in which  $\alpha$  is learning rate.

### 3. EXPERIMENTAL RESULTS

#### 3.1. Results of identifying landmarks

Figure 5 represents the identification of four landmarks types of images containing landmarks such as Figures 5(a)-5(d) matched with landmarks stored in the database and Figures 5(e)-5(h) are the resulting images with the identified landmarks (the red rectangular borders) in the indoor environment. The yellow lines show the connection between the feature points of the two landmarks in these figures. To evaluate the landmark identification performance, one can be based on the number of matching features and non-matching ones and the accuracy and error rate are calculated using the following (10) and (11):

$$R_t = \frac{TF}{SF} \times 100\% \tag{10}$$

$$R_f = \frac{SF-TF}{SF} \times 100\% \tag{11}$$

in which  $SF$  is the number of feature points of the identified landmark,  $TF$  is the number of feature points matching with the feature points of the defined landmark,  $R_t$  is the accuracy rate, and  $R_f$  is the error rate of the landmark identification process.

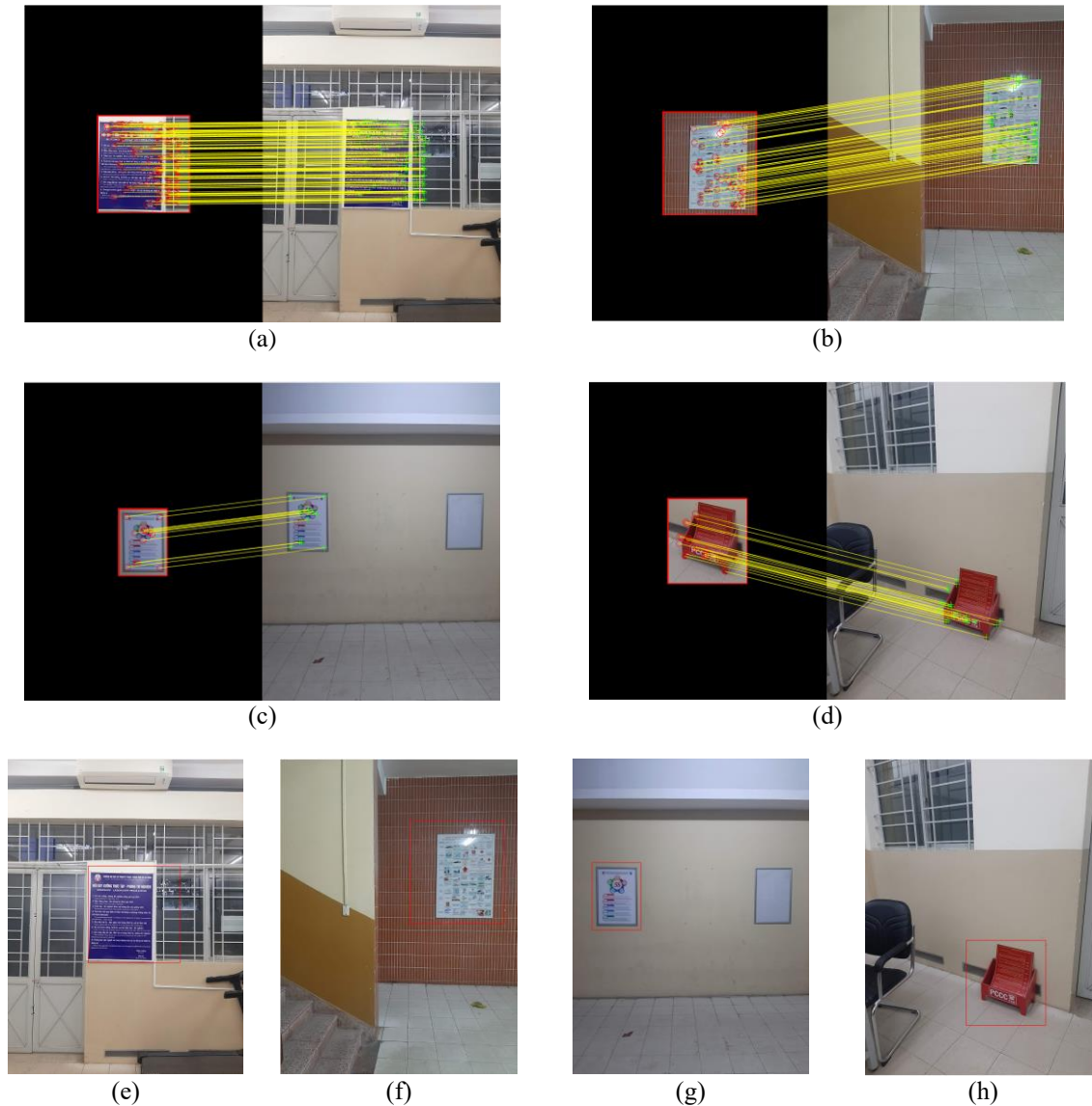


Figure 5. The representation of 4 different types of landmarks identified based on the landmarks stored in the database: (a) matching features of landmarks 1, (b) matching features of landmarks 2, (c) matching features of landmarks 3, (d) matching features of landmarks 4, (e) landmark 1 identified, (f) landmark 2 identified, (g) landmark 3 identified, and (h) landmark 4 identified

Table 1 shows that landmarks with many features (large  $SF$ ) give an accuracy rate of more than 90. Meanwhile, landmarks with few features (small  $SF$ ) have large identification errors ( $Rf > 10$ ). This indicates that the accuracy rate of landmark identification with maximum feature density is better than that of landmarks containing few feature points. In addition, Table 1 shows that the average processing time is 304 ms and this proves that the electric wheelchair and the camera system can detect landmarks during movement with high accuracy and short detection time. Once the landmark has been identified, the position information of the landmark is also provided from the collected database, serving the process of positioning the wheelchair.

Table 1. Accuracy of the identified landmarks using the SURF method

	Identification time (ms)	SF	TF	Rt (%)	Rf (%)
Figure 5(a)	370.6	206	190	92.2	7.8
Figure 5(b)	320.4	64	58	90.6	9.4
Figure 5(c)	296.9	18	13	72.2	27.8
Figure 5(d)	228.0	30	26	86.7	13.3

**3.2. Determination of the wheelchair position based on landmark**

Figure 6 depicts the accuracy of measuring the distance from the camera to the landmark. In this research, different landmarks were used for identification and distance measurement at different positions to demonstrate the accuracy of the proposed method. In particular, firstly the landmarks were horizontally placed at the same positions with the camera and then the positions of the landmarks were vertically changed. In Figure 6, the blue line represents the positions of the landmarks in the real environment and the red line represents the absolute error from the measurement. It is obvious that the horizontal distance measurement has a small error within  $\pm 1.2$  cm. Next, the landmarks are horizontally placed at a distance of 40 cm from the camera and then change its position vertically. With this experiment, the deviation of the measured distance increased to  $\pm 2.8$  cm. However, this deviation is not too large and can be acceptable.

Figure 7 shows the absolute error of the distance measurement from the camera to the landmark with different vertical distances. In Figure 7, the blue line represents the positions of the landmarks in the real environment and the red line represents the absolute error from the measurement. From this result, it is obvious that the distance measurement was more accurate when the position between the camera and the landmark is less than 1m, but it still gives an acceptable error of about  $\pm 2$  cm with a distance greater than 1m. It means that the wheelchair cannot work in a too large area.

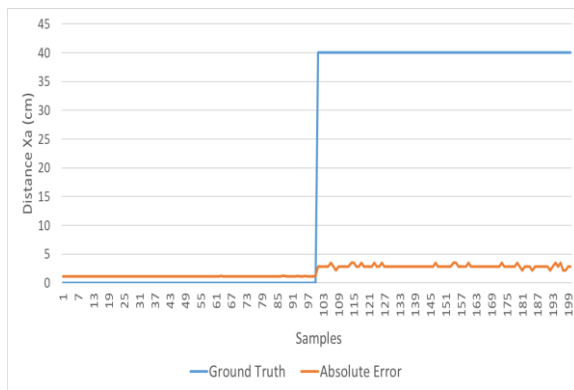


Figure 6. Absolute error of the distance  $X_a$  measurement from the camera to the landmarks at different locations

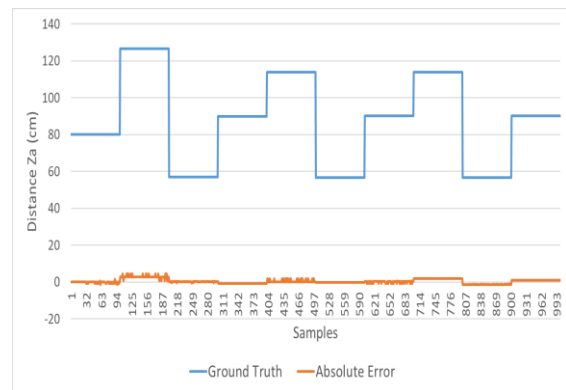
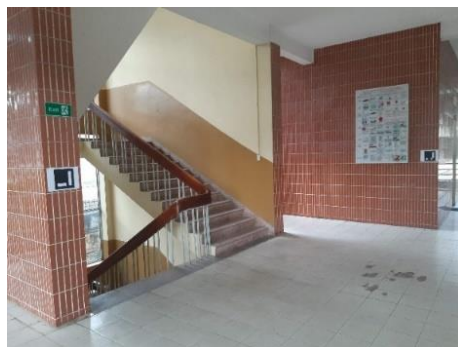
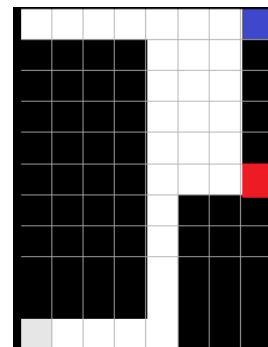


Figure 7. Absolute error of the distance  $Z_a$  measurement from the camera to the landmarks at different locations

One final experiment was performed focusing on positioning the wheelchair on a 2D grid map. In particular, the experiment was carried out in the environment with the area of  $126.72 \text{ m}^2$ , divided into the 2D grid map of the  $(8 \times 11)$  cells, in which each cell with the size of  $1.2 \times 1.2 \text{ m}$  as shown in Figure 8. The origin  $O(0,0)$  of the grid map is blue at the top left corner and the destination is a red cell with the coordinate  $C(0,5)$ . Figure 8(a) is a real environment and Figure 8(b) is a 2D grid map obtained from this environment. The experiments were performed for different positions of the wheelchair checked the accuracy of positioning on the 2D grid map based on landmarks.



(a)



(b)

Figure 8. The indoor experimental environment: (a) real environment and (b) 2D grid map

Figure 9 shows the positions of the wheelchair assigned the green icons and landmarks (yellow symbols) applied to 4 different experiments, including the landmark on the right of the grid map as Figures 9(a) and (b) and the landmark in the bottom of grid map as Figures 9(c) and 9(d). Table 2 shows the results of the wheelchair positioning on the 2D grid map with the accuracy of the experiments. In particular, after identifying the landmarks, the wheelchair determined its position in the OXY plane is  $(X_w, Y_w)$  and then the wheelchair's position on the grid map  $(X_{WG}, Y_{WG})$  is determined. In addition to identifying and calculating the wheelchair's position on the grid map, the wheelchair's orientation on the grid map is also determined based on IDs of landmarks. In this experiment, IDs of the landmarks and their directions (up, down, left, right) relative to the origin of the grid map were stored as a lookup table for easily understanding of the wheelchair's orientation. The results from Table 2 show that the absolute error of the wheelchair in the real environment can be acceptable and the wheelchair can accurately determine its position on the grid map.

Figure 10 shows wheelchair positions (green icons) and landmarks are assigned to be yellow icons in two different experiments: the wheelchair at position (3,3) in the grid map as shown in Figure 10(a) and the position (3,2) as shown in Figure 10(b). Table 3 shows the results of the wheelchair positioning on a 2D grid map made by the wheelchair positioning method to determine the accuracy [30]. In particular, after identifying three landmarks and measuring the distance from the wheelchair to the landmarks, the wheelchair position was calculated in the OXY plane as  $(X_w, Y_w)$ , then the wheelchair position on grid map  $(X_{WG}, Y_{WG})$  was determined. The results from Table 3 show that the absolute error of the wheelchair in the real environment using three landmarks is larger than when using one landmark. Moreover, in this experiment, if all three landmarks lie on the same plane or the system can not find all three landmarks, its position can not be located. Therefore, this is a limitation of the method using three landmarks compared to one landmark in this research.

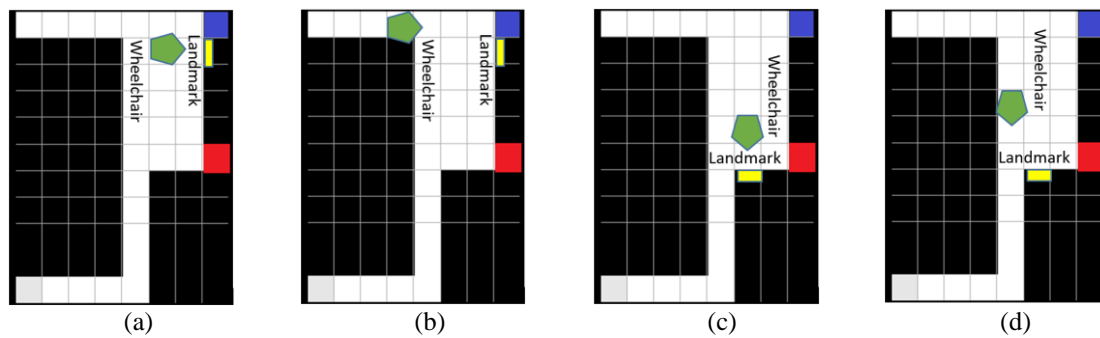


Figure 9. Four positions of the wheelchair on the 2D grid map with the landmarks: (a) the 1<sup>st</sup> position, (b) the 2<sup>nd</sup> position, (c) the 3<sup>rd</sup> position, and (d) the 4<sup>th</sup> position

Table 2. Accuracy of positioning the wheelchair

No.	Real position $(X_0, Y_0)$	Calculated position $(X_w, Y_w)$	$ X_w - X_0 $ (cm)	$ Y_w - Y_0 $ (cm)	Position on 2D grid map $(X_{WG}, Y_{WG})$	Wheelchair direction on 2D grid map
1	(180, 720)	(182, 718)	2	2	(2,1)	Up
2	(60, 480)	(58, 477)	2	3	(4,0)	Up
3	(600, 660)	(596, 665)	4	5	(2,4)	Right
4	(480, 540)	(474, 538)	6	2	(3,3)	Right

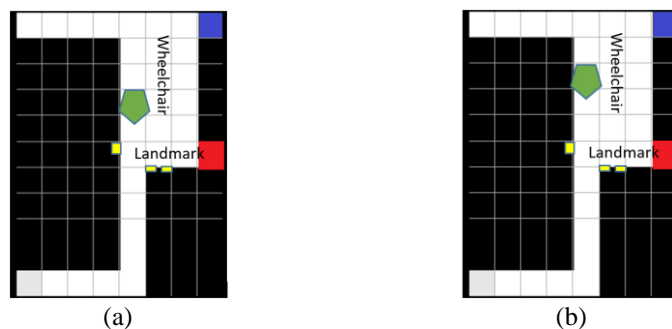


Figure 10. Positions of the wheelchair on the 2D grid map with 3 landmarks (yellow): (a) the wheelchair at the position (3,3) and (b) the wheelchair at the position (3,2)

Table 3. Accuracy of positioning the wheelchair using 3 landmarks

No.	Real position ( $X_0, Y_0$ )	Calculated position ( $X_w, Y_w$ )	$ X_w - X_0 $ (cm)	$ Y_w - Y_0 $ (cm)
1	(480, 540)	(489, 564)	8	14
2	(360, 540)	(348, 534)	12	6

**3.3. Movement wheelchair based on its determined position and Q-learning**

The wheelchair is installed to move at the speed of 3 km/h to match the system’s processing performance. The experimental environment as depicted as shown in Figure 11, in which the wheelchair was placed at the position A(4,0) as shown in Figure 11(a) to reach the desired destination C(0,5). To begin the moving process, the wheelchair identified the landmark and then determined its position and orientation on the grid map. The Q-learning method was applied to suggest a route for the wheelchair movement to the pre-established destination as shown in Figure 11(a). Therefore, the system provides a chain of commands to directly control the wheelchair with commands including forward, left, right, backward to steer according to the simulated route as described in Table 4.

Table 4. Wheelchair control commands converted from the simulated commands

State of wheelchair	Current direction $d$	Action of model $a$	New direction $d'$	Action of wheelchair $a_w$
(4,0) to (3,0)	Up	Up	Up	Forward
(3,0) to (2,0)	Up	Up	Up	Forward
(2,0) to (1,0)	Up	Up	Up	Forward
(1,0) to (1,0)	Up	Right	Right	Right-Forward
(1,1) to (1,2)	Right	Right	Right	Forward
(1,2) to (1,3)	Right	Right	Right	Forward
(1,3) to (1,4)	Right	Right	Right	Forward
(1,4) to (1,5)	Right	Right	Right	Forward
(1,5) to (0,5)	Right	Up	Up	Left-Forward

From Figure 11(b), it can be seen that the actual path of the wheelchair is redrawn as it moved from the starting point A(4,0) to destination C(0,5) on the grid map. In particular, the wheelchair moved along the blue line and followed the red reference line. This result shows that the system of the electric wheelchair positioned based on the landmark can move to the desired destination based on the proposed path using the Q-learning method.

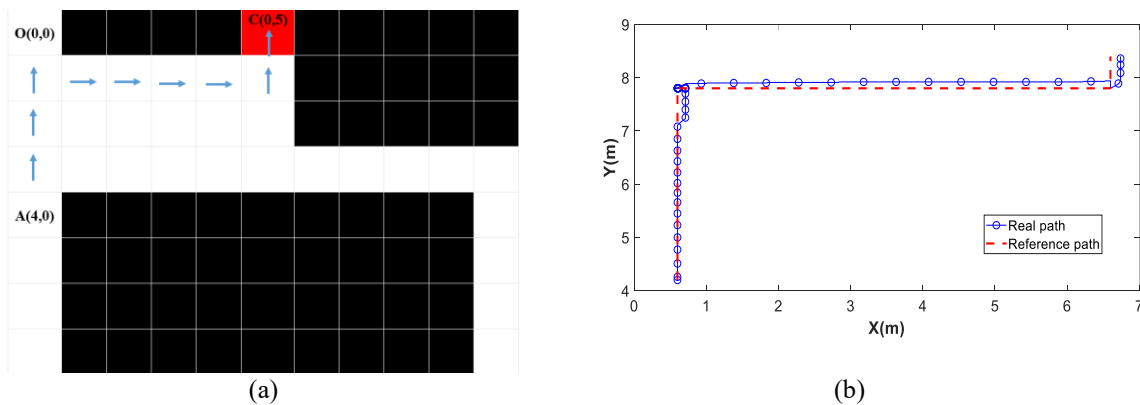


Figure 11. Wheelchair path: (a) simulated path with the start and destination points and (b) actual path of the wheelchair

**4. CONCLUSION**

In the paper, landmarks were used to position the electric wheelchair in the 2D grid map. In particular, some experiments have been carried out to demonstrate that the landmark system was used for wheelchair navigation in an indoor environment. The results showed that the localization accuracy was affected by the position of the landmarks and the distance between the wheelchair and the landmark. From these experiments,

the RGB-D camera system is a good choice in this study because of its low cost, popularity, and ease of development with good resolution to provide 3D information of indoor environments. In addition, we showed that wheelchair activity based on landmarks can be good in small areas, such as rooms, where a sufficient distance can be easily ensured for the identification of landmarks. Moreover, the error when determining the position depends only on the conditions ensuring the ability to identify landmarks by using this camera system and does not depend on time. In addition, our research showed that it is reliable for applying the proposed method with Q-learning for navigation of the wheelchair on the 2D grid map.

## ACKNOWLEDGEMENTS

We would like to thank Ho Chi Minh City University of Technology and Education (HCMUTE), Vietnam.

## REFERENCES

- [1] R. Hassani, M. Boumehraz, and M. Hamzi, "Implementation of wheelchair controller using mouth and tongue gesture," *Indonesian Journal of Electrical Engineering and Computer Science (IJECS)*, vol. 24, no. 3, pp. 1663-1671, 2021, doi: 10.11591/ijeecs.v24.i3.pp1663-1671.
- [2] E. F. Lopresti, V. Sharma, R. C. Simpson, and L. C. Mostowy, "Performance testing of collision-avoidance system for power wheelchairs," *Journal of Rehabilitation Research and Development*, vol. 48, no. 5, pp. 529-544, 2011, doi: 10.1682/jrrd.2010.01.0008.
- [3] M. Babel *et al.*, "Assessment of a navigation assistance system for power wheelchair," *Annals of Physical and Rehabilitation Medicine*, vol. 58, pp. 58-99, 2015, doi: 10.1016/j.rehab.2015.07.241.
- [4] V. Sharma, R. C. Simpson, E. F. LoPresti, and M. Schmeler, "Clinical evaluation of semiautonomous smart wheelchair architecture (Drive-Safe System) with visually impaired individuals," *Journal of Rehabilitation Research and Development*, vol. 49, no. 1, pp. 35-50, 2012, doi: 10.1682/jrrd.2010.03.0022.
- [5] R. Gonzalez, F. Rodriguez, J. L. Guzman, and M. Berenguel, "Comparative study of localization techniques for mobile robots based on indirect Kalman filter," in *Proceedings of IFR Int. Symposium on Robotics*, 2009, pp. 253-258.
- [6] M. Drumheller, "Mobile robot localization using sonar," *IEEE Transactions on Pattern Analysis and Machine Intelligence*, vol. PAMI-9, no. 2, pp. 325-332, 1987, doi: 10.1109/TPAMI.1987.4767907.
- [7] H. Joachim and R. Joachim, "Localization of a mobile robot by matching 3D-laser-range-images and predicted sensor images," in *Proceedings of the Intelligent Vehicles '94 Symposium*, 1994, pp. 345-350, doi: 10.1109/IVS.1994.639542.
- [8] R. M. Ramli *et al.*, "Development of robotic rover with controller and vision systems," *Indonesian Journal of Electrical Engineering and Computer Science (IJECS)*, vol. 18, no. 2, pp. 766-773, 2020, doi: 10.11591/ijeecs.v18.i2.pp766-773.
- [9] Y. Xu *et al.*, "Design and recognition of monocular visual artificial landmark based on arc angle information coding," in *33rd Youth Academic Annual Conference of Chinese Association of Automation (YAC)*, 2018, pp. 722-727, doi: 10.1109/YAC.2018.8406466.
- [10] A. M. G. Pinto, A. P. Moreira, and P. G. Costa, "Indoor localization system based on artificial landmarks and monocular vision," *TELKOMNIKA (Telecommunication Computing Electronics and Control)*, vol. 10, no. 4, pp. 609-620, 2012, doi: 10.12928/telkomnika.v10i4.848.
- [11] S. Hwang and J. Song, "Monocular vision-based SLAM in indoor environment using corner, lamp, and door features from upward-looking camera," *IEEE Transactions on Industrial Electronics*, vol. 58, pp. 4804-4812, 2011, doi: 10.1109/TIE.2011.2109333.
- [12] J. Vidal and C. Lin, "Simple and robust localization system using ceiling landmarks and infrared light," in *12th IEEE International Conference on Control and Automation (ICCA)*, 2016, pp. 583-587, doi: 10.1109/ICCA.2016.7505340.
- [13] M. Guo *et al.*, "3D lidar SLAM based on ground segmentation and scan context loop detection," in *IEEE 11th Annual International Conference on CYBER Technology in Automation, Control, and Intelligent Systems (CYBER)*, 2021, pp. 692-697, doi: 10.1109/CYBER53097.2021.9588285.
- [14] X. Chai, F. Wen, and K. Yuan, "Fast vision-based object segmentation for natural landmark detection on indoor mobile robot," in *IEEE International Conference on Mechatronics and Automation*, 2011, pp. 2232-2237, doi: 10.1109/ICMA.2011.5986286.
- [15] S. Manen, M. Guillaumin, and L. V. Gool, "Prime object proposals with randomized prim's algorithm," in *IEEE International Conference on Computer Vision*, 2013, pp. 2536-2543, doi: 10.1109/ICCV.2013.315.
- [16] C. H. Lampert, M. B. Blaschko, and T. Hofmann, "Beyond sliding windows: Object localization by efficient subwindow search," in *IEEE Conference on Computer Vision and Pattern Recognition*, 2008, pp. 1-8, doi: 10.1109/CVPR.2008.4587586.
- [17] B. Alexe, T. Deselaers, and V. Ferrari, "Measuring the objectness of image windows," *IEEE Transactions on Pattern Analysis and Machine Intelligence*, vol. 34, no. 11, pp. 2189-2202, 2012, doi: 10.1109/TPAMI.2012.28.
- [18] J. Carreira and C. Sminchisescu, "CPMC: automatic object segmentation using constrained parametric min-cuts," *IEEE Transactions on Pattern Analysis and Machine Intelligence*, vol. 34, no. 7, pp. 1312-1328, 2012, doi: 10.1109/TPAMI.2011.231.
- [19] B.-V. Ngo and T.-H. Nguyen, "Dense feature-based landmark identification for mobile platform localization," *International Journal of Computer Science and Network Security*, vol. 18, pp. 186-200, 2018.
- [20] I. Endres and D. Hoiem, "Category-independent object proposals with diverse ranking," *IEEE Transactions on Pattern Analysis and Machine Intelligence*, vol. 36, no. 2, pp. 222-234, 2014, doi: 10.1109/TPAMI.2013.122.
- [21] J. R. Uijlings, K. E. Sande, T. Gevers, and A. W. Smeulders, "Selective search for object recognition," *International Journal of Computer Vision*, vol. 104, pp. 154-171, 2013, doi: 10.1007/s11263-013-0620-5.
- [22] S. Se, D. Lowe, and J. Little, "Vision-based mobile robot localization and mapping using scale-invariant features," in *Proceedings 2001 ICRA. IEEE International Conference on Robotics and Automation*, 2001, vol. 2, pp. 2051-2058, doi: 10.1109/ROBOT.2001.932909.
- [23] H. Zhang, S. Jianzhu, L. Zhang, and J. Dai, "Landmark-based localization for indoor mobile robots with stereo vision," *Intelligent System Design and Engineering Application (ISDEA), 2012 Second International Conference*, 2012, pp. 700-702, doi: 10.1109/ISdea.2012.640.
- [24] D. C. Herath, S. Kodagoda, and G. Dissanayake, "Simultaneous localisation and mapping: a stereo vision based approach," *Intelligent Robots and Systems, 2006 IEEE/RSJ International Conference*, 2006, pp. 922-927, doi: 10.1109/IROS.2006.281749.

- [25] K.-H. Lin and C.-C. Wang, "Stereo-based simultaneous localization, mapping and moving object tracking," *Intelligent Robots and Systems (IROS), 2010 IEEE/RSJ International Conference*, 2010, pp. 3975-3980, doi: 10.1109/IROS.2010.5649653.
- [26] J.S. Chiang, C.-H. Hsia, and H.-W. Hsu, "A stereo vision-based self-localization system," *IEEE Sensors Journal*, vol. 13, no. 5, pp. 1677-1689, 2013, doi: 10.1109/JSEN.2013.2240449.
- [27] B.-V. Ngo and T.-H. Nguyen, "A semi-automatic wheelchair with navigation based on virtual-real 2D grid maps and EEG signals," *Applied Sciences*, vol. 12, pp. 8880, 2022, doi: 10.3390/app12178880.
- [28] S. N. Reddy and J. Mungara, "Received signal strength indication based clustering and aggregating data using Q-learning in mobile Ad Hoc network," *Indonesian Journal of Electrical Engineering and Computer Science (IJECS)*, vol. 27, no. 2, pp. 867-875, 2022, doi: 10.11591/ijeecs.v27.i2.pp867-875.
- [29] S. M. Hussain, K. M. Yusof, R. Asuncion, and S. Hussain "Artificial intelligence based handover decision and network selection in heterogeneous internet of vehicles," *Indonesian Journal of Electrical Engineering and Computer Science (IJECS)*, vol. 22, no. 2, pp. 1124-1134, 2021, doi: 10.11591/ijeecs.v22.i2.pp1124-1134.
- [30] N. T. Nhu and N. T. Hai, "Landmark-based robot localization using a stereo camera system," *American Journal of Signal Processing*, vol. 5, no. 2, pp. 40-50, 2015, doi: 10.5923/j.ajsp.20150502.03.

## BIOGRAPHIES OF AUTHORS



**Ba-Viet Ngo**    received his M.Eng. degree in electronics engineering from HCMC University of Technology and Education in 2014. He is a Ph.D. student in electronics engineering at HCM City University of Technology and Education. His research interests include smart wheelchair, artificial intelligence, and image processing. He can be contacted at email: vietnb@hcmute.edu.vn.



**Thanh-Hai Nguyen**    received his B.Eng. degree with electronics engineering from the HCMC University of Technology and Education (HCMUTE), Vietnam, 1995; M.Eng. degree with telecommunication and electronics engineering from HCMC University of Technology (HCMUT), in Vietnam, 2002; Ph.D. degree with electronics engineering from university of technology, Sydney (UTS) in Australia, 2010. Currently, he is a lecturer in the department of industrial electronic-biomedical engineering, faculty of electrical-electronics engineering, HCMUTE, Vietnam. His research interests are Bio-signal and image processing, machine learning, smart wheelchairs and artificial intelligence. He can be contacted at email: nthai@hcmute.edu.vn.